Helimagnetic order in ferric arsenate, $FeAsO_4$

1999 J. Phys.: Condens. Matter 11 1473

(http://iopscience.iop.org/0953-8984/11/6/011)

J. Phys.: Condens. Matter **11** (1999) 1473–1478. Printed in the UK PII: S0953-8984(99)98373-X

Helimagnetic order in ferric arsenate, $FeAsO_4$

J B Forsyth†‖, J P Wright‡, M D Marcos‡, J P Attfield‡ and C Wilkinson§

† Rutherford Appleton Laboratory, Chilton, Oxfordshire OX11 0QX, UK
‡ Department of Chemistry, University of Cambridge, Lensfield Road, Cambridge CB2 1EW, UK
§ European Molecular Biology Laboratory, Grenoble, France

Received 14 October 1998, in final form 3 December 1998

Abstract. High-resolution time of flight neutron powder diffractometry has been used to determine the antiferromagnetic structure of ferric arsenate at 4.2 K. The structure is incommensurate with a magnetic propagation vector (0.04994(3), 0, −0.24725(2)) in the a^*–c^* plane of the monoclinic unit cell. The spins of 4.01(2) μ_B on the Fe^{3+} ions rotate in a plane containing b^* and making an angle of 34.1(7)° to [001] in β obtuse. The structure shows that the dominant antiferromagnetic coupling is between Fe^{3+} ions which are linked through tetrahedral arsenate groups giving a frustrated exchange network.

1. Introduction

Ferric arsenate is one of the few known examples of five-coordinate high-spin iron (III) in an oxyanion network system. The preparation of $FeAsO_4$ was first reported by Schafer *et al* [1] in 1956, and the crystal structure was determined in 1986 from high-resolution neutron powder diffraction data [2]. More precise structural parameters were obtained from a single-crystal x-ray study by Reiff *et al* [3]. The structure is illustrated in figure 1. These authors [3] also reported low-temperature magnetic susceptibility data and Mössbauer spectra which show that three-dimensional antiferromagnetic ordering is established below 67.5 K.

We now describe a high-resolution time of flight neutron powder study of $FeAsO_4$ which has enabled us to determine the incommensurate antiferromagnetic structure stable at 4.2 K. The details of this structure are discussed in relation to the magnetic exchange paths within the crystal.

2. Experiment

The specimen of $FeAsO_4$ was prepared by dissolving stoichiometric quantities of $Fe(NO)_3 \cdot 9H_2O$ (Aldrich ACS) and $As_2O_5 \cdot xH_20$ ($x \sim 3$, Aldrich) in dilute nitric acid and boiling the solution to dryness. The residue was ground and heated to 800 °C in air to give an off-white powder product whose x-ray powder diffraction pattern showed no impurity lines.

The first neutron powder diffraction data were obtained using the D1A instrument at the Institut Laue Langevin, Grenoble, France. Figure 2 shows the low-angle portion of the 4.2 K pattern obtained using an incident wavelength of 2.98 Å. Unfortunately, the instrumental resolution made it difficult to determine the number of peaks contributing to the low-angle magnetic intensity in the 2θ range 22–28° and the magnetic propagation vector was not determined.

‖ Now at the Clarendon Laboratory, Parks Road, Oxford OX1 3PU, UK.

0953-8984/99/061473+06$19.50

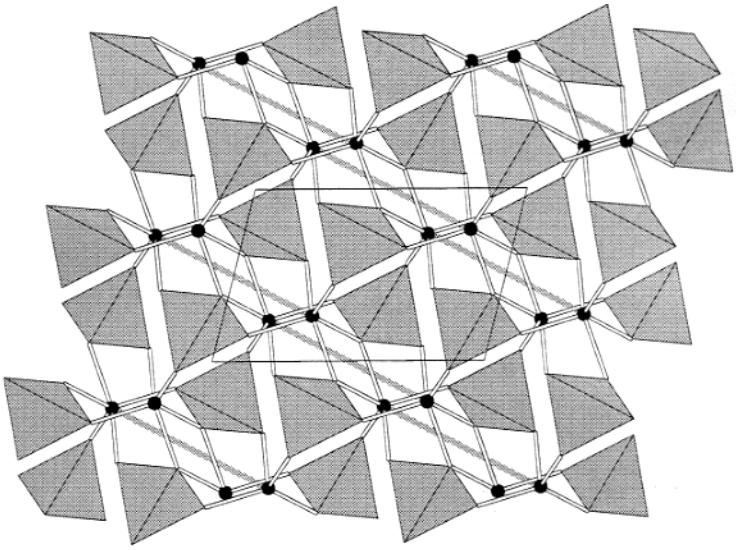

Figure 1. The crystal structure of ferric arsenate [3] projected down [010]. The antiferromagnetically coupled dimers are highlighted, the Fe^{3+} ions are shown as black spheres and the AsO_4 groups as tetrahedra.

Subsequently, a second data set was obtained using the diffraction detector of the IRIS high-resolution inelastic spectrometer at the ISIS pulsed neutron facility. This provides a $\Delta d/d$ resolution of 2.5×10^{-3} which extends to $d \sim 12$ Å and proved sufficient to allow the propagation vector to be found. Some 10 g of the powder with particle size less than 150 μm were sealed in a thin-walled aluminium sample can of rectangular cross section $40 \times 40 \times 4$ mm and oriented so that the minor dimension of the can was parallel to the incident neutron beam in an Orange liquid He cryostat. This geometry was chosen to optimize the diffracted intensity into a backward-angle bank of ten closely spaced 0.5 in diameter ^{3}He detectors which form the diffraction detector on IRIS. The detection system is 850 mm from the sample, at which it subtends a solid angle of 0.018 steradians, and covers a range of 166–172° in 2θ.

Time of flight data were collected at 25 Hz repetition rate in a series of d-spacing ranges 2.3–3.9, 3.4–5.0, 4.85–6.45, 6.0–7.6, 7.2–8.8, 8.4–10.0 and 9.65–11.25 Å to avoid frame overlap due to the long incident path length of 36 m. Data were collected for total incident proton beam currents of 90, 150, 210, 270, 283, 260 and 300 μA hours, respectively to provide similar counting statistics in every range. Subsequent data analysis showed that six of the ten detector chains had been subject to externally generated noise pulses and their data were rejected. The data from the remaining four detectors were combined to form a focused data set. After normalization using the spectra from a main beam monitor and correction for the wavelength dependence of the detector, the spectral ranges were finally merged to provide a composite pattern covering the range 40 to 143 ms time of flight, equivalent to 2.3 to 7.6 Å in d-spacing. No diffraction peaks were observed at longer d-spacings up to the limit of observation at 11.25 Å.

3. Determination of the magnetic structure

The incommensurate nature of the magnetic ordering in $FeAsO_4$ became evident through failure to index the strong magnetic peaks at large d-spacing on the basis of the chemical

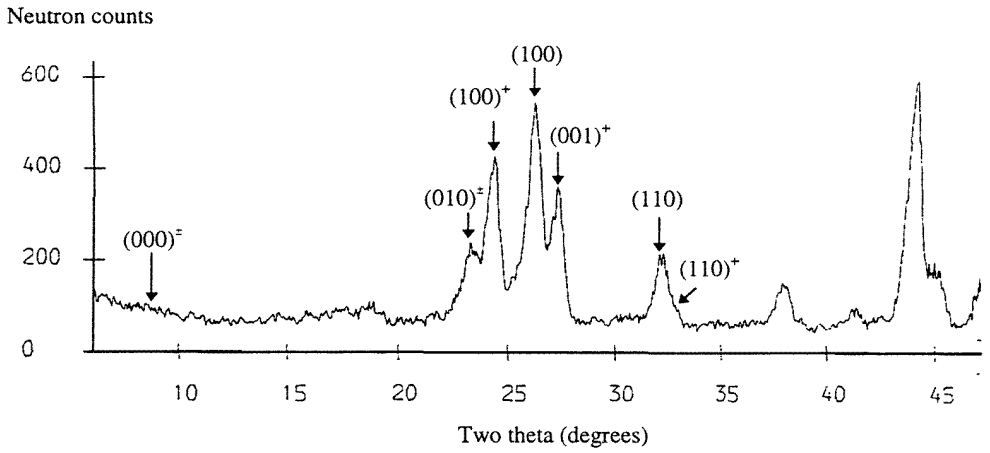

Figure 2. Low-angle portion of the powder diffraction profile of $FeAsO_4$ obtained at 4.2 K using D1A. The position of the $(000)^{\pm}$ reflections corresponding to a magnetic propagation vector (0.050, 0, −0.247) is arrowed.

unit cell or simple multiples of its dimensions. The incommensurate magnetic propagation vector was determined by two independent methods; firstly using the method developed by Wilkinson *et al* to determine the propagation vector in $MnWO_4$ [4], and secondly through an exhaustive indexing of the first three magnetic peaks. In the latter method, indexing one magnetic satellite peak as $(000)^{\pm}$ and assigning indices to two others allows the corresponding propagation vector to be derived analytically. By indexing the longest d-spacing peak as the $(000)^{\pm}$ satellite and the next two peaks as satellites of all the permutations of structural peaks in the first Brillouin zone, an exhaustive list of possible propagation vectors was created. A computer program was written to test which of these could index the rest of the magnetic peaks in the observed data set and a single propagation vector of $\pm(-0.050, \pm 1.000, 0.248)$ was found. Translating this vector back into the first Brillouin zone gives essentially the same solution as the Wilkinson search process. It was noticeable that the Wilkinson solution did not, however, produce as good a fit to the observed d-spacings of six well resolved magnetic peaks as that which had been obtained in previous analyses of time-of flight data from IRIS. This was subsequently explained by the relative lack of precision in the unit cell dimensions at 4.2 K due to the paucity of nuclear peaks in the restricted range of long d-spacing data available. Nevertheless, the trial propagation vector of (0.044, 0, −0.243) was sufficiently accurate to enable the observed data to be indexed and to show that there was no observable intensity at the positions of the reflections $(101)^{\pm}$ and $(\bar{1}01)^{\pm}$ which lie within the same range of d. Moreover, the $(000)^{\pm}$ peak was also found to be absent in the D1A data (figure 2).

The chemical unit cell of $FeAsO_4$ contains four symmetry related Fe^{3+} ions in a general position in space group $P2_1/n$. The positions of the Fe^{3+} ions within the chemical cell were labelled as:

Fe1	x	y	z
Fe1′	$-x$	$-y$	$-z$
Fe2	$\frac{1}{2}+x$	$\frac{1}{2}-y$	$\frac{1}{2}+z$
Fe2′	$\frac{1}{2}-x$	$\frac{1}{2}+y$	$\frac{1}{2}-z$

where $x = 0.1751$, $y = 0.4603$ and $z = 0.7631$ from Reiff *et al* [3]. We assume that the iron

Table 1. Phases φ and their esds for the Fe^{3+} moments within the chemical unit cell from the profile refinement. The phase of Fe1 is arbitrarily set to zero and the phase of Fe2 is determined solely by the magnetic propagation vector and the anti n glide.

Atom	x	y	z	φ (°)
Fe1	0.1751	0.4603	0.7631	0
Fe1′	0.8249	0.5397	0.2369	265.5(4)
Fe2	0.6751	0.9603	0.2631	233.5
Fe2′	0.3249	0.0397	0.7269	32.0(4)

moment directions form a spiral and can be described by a function

$$\boldsymbol{\mu}_{lj} = \boldsymbol{u}\cos(2\pi\boldsymbol{k}\cdot\boldsymbol{R}_l + \phi_j) + \boldsymbol{v}\sin(2\pi\boldsymbol{k}\cdot\boldsymbol{R}_l + \phi_j)$$

where $\boldsymbol{\mu}_{lj}$ is the moment on atom j (of the four) in a unit cell translated by a lattice vector $\boldsymbol{R}_l$ from the origin. $\boldsymbol{k}$ is the propagation vector, $\boldsymbol{u}$ and $\boldsymbol{v}$ are orthogonal vectors and ϕ_j is a phase shift associated with atom j. The absence of magnetic satellites to the (000), ($\bar{1}$01) and (101) reflections is consistent with the n glide being an anti-operator in the magnetic arrangement which forms the basis of the helix. Associating a phase shift of $\Delta\phi_{12} = 2\pi(\boldsymbol{k}\cdot\boldsymbol{r}_{12} + \frac{1}{2})$ for the relative phases of pairs of ions Fe1 and Fe2 where $\boldsymbol{r}_{12}$ is the vector relating Fe1 to Fe2 and similarly $\Delta\phi_{1'2'} = 2\pi(\boldsymbol{k}\cdot\boldsymbol{r}_{1'2'} + \frac{1}{2})$ for the pair Fe1′ and Fe2′ causes the required intensities to be zero. The phase shift between the moment on Fe1 and that on the centrosymmetrically related atom Fe1′ remained to be determined.

Structural refinement was carried out using the Rietveld program TF112M based on the Cambridge Crystallography Subroutine Library (CCSL) [5]. This program allows the propagation vector to be refined and provides for differences in shape between peaks of nuclear and magnetic origin, as well as all the usual parameters. Experience has shown that the correlation length in many helical structures is such that the magnetic peaks are significantly broader than the nuclear ones. The calculated spectra were corrected for the specimen absorption and scattering. The model used structural parameters from [3] and cell parameters obtained in the refinement of the propagation vector. Initially, it was assumed that the helical components $\boldsymbol{u}$ and $\boldsymbol{v}$ were equal in magnitude and the moments were constrained to lie in the plane perpendicular to [001]. Although this model produces the correct magnetic absences, allowing the moment value and the relative phase shift of the two pairs of atoms to refine still resulted in significant intensity mismatches for the magnetic peaks which suggested that the plane in which the moments rotate should be rotated around [010]. The refinement then proceeded rapidly to a final profile R factor of 7.83% with $\chi^2 = 5.17$. The phases of the moments on the Fe^{3+} ions relative to that on Fe1 are also given in table 1. Removing the constraint on the phase of Fe2 produced no significant improvement in the profile R factor and it was also not possible to obtain a satisfactory fit with the moment directions ($\boldsymbol{u}$ and $\boldsymbol{v}$) in the $\boldsymbol{ac}$-plane.

Removing the equality constraint on the orthogonal components of the moment, $\boldsymbol{u}$ and $\boldsymbol{v}$, did not produce a significant improvement in the fit indicating that the spiral is not significantly elliptical. Although the program allows for different profile function parameters for the nuclear and magnetic peaks, no significant improvement in the profile fit could be obtained by allowing the peak descriptions to differ. This indicates that the coherence length of the magnetic spiral is similar to the crystallite size.

The refined values of the propagation vector and the unit cell parameters are: (0.049 94(3), 0, −0.247 25(2)) and $a = 7.5609(1)$, $b = 8.075\,65(8)$, $c = 5.0907(2)$ Å, $\beta = 104.4492(7)^\circ$, respectively. The Fe^{3+} magnetic moment is 4.01(2) μ_B and the plane in which spins rotate

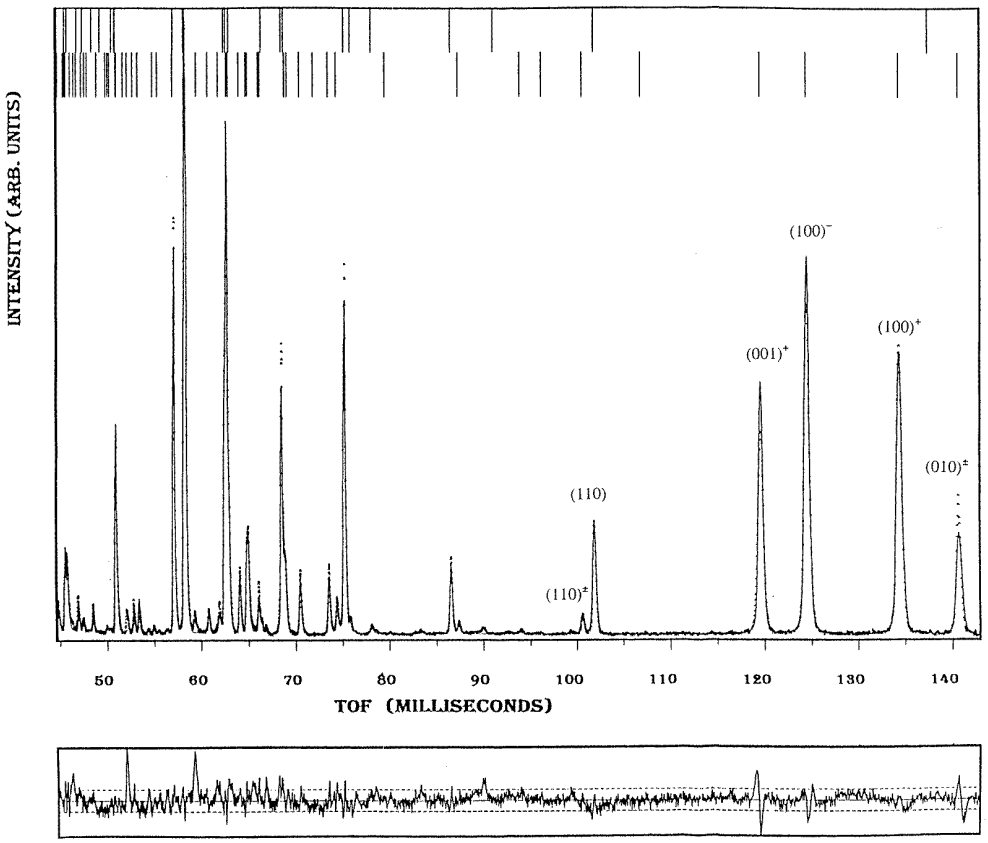

Figure 3. Profile fit to the observed time of flight diffraction pattern of $FeAsO_4$. The upper and lower sets of vertical bars mark the calculated positions of nuclear and magnetic reflections, respectively. The lower box shows the difference between the observed and calculated profiles divided by the esd, σ, in the measured profile: the broken lines are at $\pm 3\sigma$.

contains $\boldsymbol{b}$ and a vector in the $\boldsymbol{ac}$ plane 34.1(7)° from [001] in β obtuse. Figure 3 illustrates the excellent fit between the observed and calculated time of flight neutron spectrum for this model. The model predicts no diffraction peaks with d greater than 7.5 Å, so the observations beyond 7.6 Å have not been included in the figure, since they were featureless.

4. Discussion

The magnetic structure is illustrated in figure 4. Many of the interactions are almost fully frustrated with spins having relative orientations which make them almost orthogonal. The dominant interaction appears to be between Fe^{3+} sites which are linked via almost linear –O–As–O– bridges and it is this frustration of the interactions between these pairs which gives rise to the incommensurate structure. These pairs are highlighted in figure 1. The plane in which the magnetic moments rotate appears to bear no relation to the direction of the propagation vector, which makes an angle of 158° to [001] in β obtuse, compared to the angle of 34.1(6)° for the plane in which the moments rotate. The Fe–O–Fe linked dimers, postulated by Reiff *et al* [3] as being strongly antiferromagnetic, have relative spin orientations of 112.5°

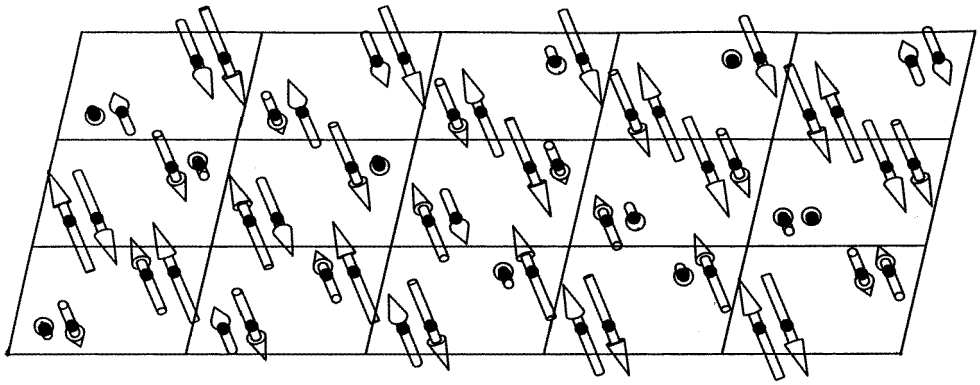

Figure 4. Magnetic structure of $FeAsO_4$ projected down [010], with the a-axis horizontal.

suggesting that this particular coupling is in fact weak, perhaps because of competing potential superexchange and direct exchange interactions between the Fe–O–Fe linked ions. The refined moment value of 4.01(2) μ_B is reduced from the ideal value of 5.0 μ_B for high-spin Fe^{3+} which reflects the degree of frustration present in the structure.

The refinement of the low-temperature nuclear structure was not possible with this data set and room-temperature parameters were used; it would therefore be highly desirable to carry out further measurements over a greater range of d-spacing to determine precise magnetic and structural parameters simultaneously. This highly frustrated magnetic structure illustrates the complexity of magnetic structure which can now be tackled with high-resolution time of flight neutron powder diffraction and particularly highlights the applicability of these methods to the precise determination of complex propagation vectors.

Acknowledgments

We thank EPSRC for provision of neutron beam time and also M James and M A Adams for assistance with the data collection. JPW thanks EPSRC for a CASE studentship in association with RAL. We are also grateful to the British Council and the Ministerio de Educacion y Ciencia for an Acciones Integradas award, and for an FPIE fellowship from the latter organization for MDM.

References

[1] Shafer E C, Shafer M W and Roy R 1956 *Z. Kristallogr.* **108** 263
[2] Cheetham A K, Jakeman R J B, David W I F, Eddy M M, Johnson M W and Torardi C C 1986 *Nature* **320** 46
[3] Reiff W M, Kwiecien M J, Jakeman R J B, Cheetham A K and Torardi C C 1993 *J. Solid State Chem.* **107** 401
[4] Wilkinson C, Lautenschlager G, Hock R and Weitzel H 1991 *J. Appl. Crystallogr.* **24** 365
[5] Matthewman J C, Thompson P and Brown P J 1982 *J. Appl. Crystallogr.* **15** 167